Supplementary Information to

The influence of cellular energy status, microtubules, and crowding on mitochondrial motion

Beatrice Corci,[a,b] Werner J. H. Koopman,[c,d,e] Amalia M. Dolga,[a] Christoffer Åberg[a*]

[a] Groningen Research Institute of Pharmacy, University of Groningen, Antonius Deusinglaan 1, 9713 AV Groningen, The Netherlands.
[b] Zernike Institute for Advanced Materials, University of Groningen, Nijenborgh 3, 9747 AG Groningen, The Netherlands.
[c] Department of Pediatrics, Amalia Children's Hospital, Radboud University Medical Center, Nijmegen, The Netherlands.
[d] Radboud Center for Mitochondrial Medicine, Radboud University Medical Center, Nijmegen, The Netherlands.
[e] Human and Animal Physiology, Wageningen University & Research, Wageningen, The Netherlands.

[*] christoffer.aberg@rug.nl

Supplementary methods

Mitochondrial network analysis

To evaluate changes in the mitochondrial network in perturbed cells, the ImageJ plugin Mitochondria Analyzer[1] was used. To allow application of the plugin, the raw microscopy images of MitoTracker-stained mitochondria were converted from 16 to 8-bit images, and subsequently the background was removed by subtracting from the image the mean fluorescence value of a small region of interest outside of the cells. The processed images were then thresholded with the plugin, using a weighted mean method and a block size of 1.25 µm and a C-value of 5 (for details on the choice of threshold parameters see previous literature[2]). The same threshold parameters were used for all conditions. Seven parameters were chosen for the analysis: morphologic descriptors (area, perimeter, form factor, aspect ratio) and network descriptors (branches, mean branch length, branch junctions). All of them were determined on a per-mito basis and later averaged over mitochondria.

Supplementary figures

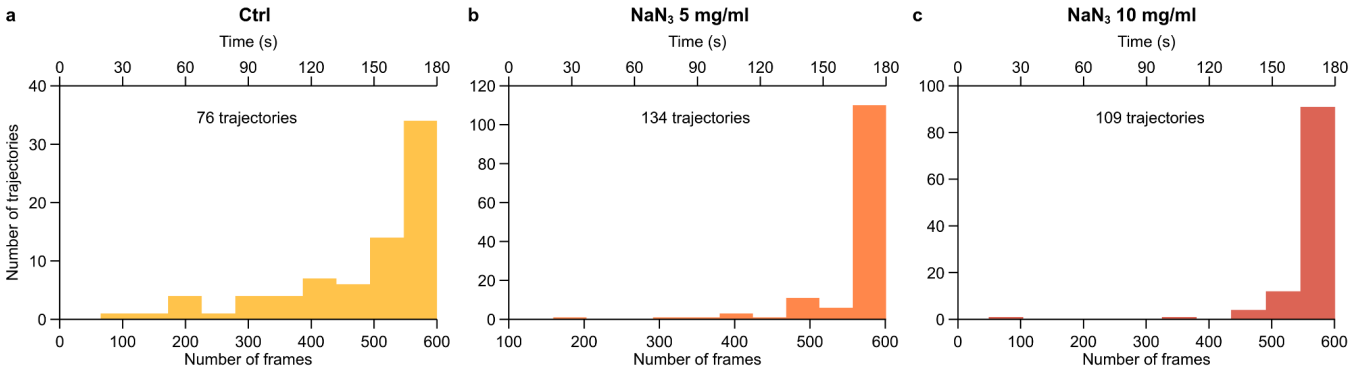

Figure S1. Trajectory length distributions of tracked mitochondria in cell energy-depleted HEK 293 cells. It was not always possible to track mitochondria for the entire duration of the acquired microscopy images (600 frames or 3 min) so here we present the actual lengths of the acquired trajectories. (a) Control (unperturbed) cells; (b) Cells exposed to 5 mg/ml sodium azide for 3 h; and (c) Cells exposed to 10 mg/ml sodium azide for 3 h. The results are presented both in terms of frames (lower *x* axes) as well as time (upper *x* axes). The number of trajectories is also specified for each condition.

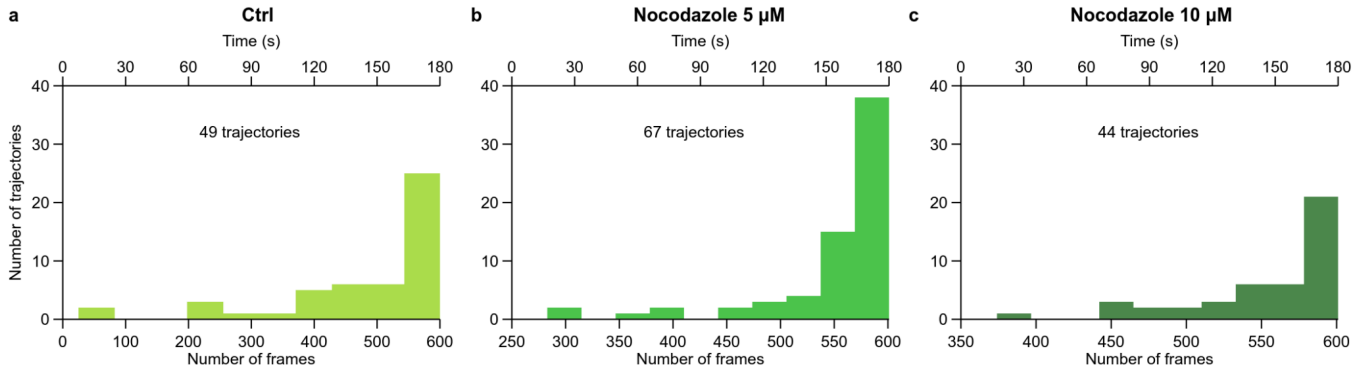

Figure S2. Trajectory length distributions of tracked mitochondria after microtubule disruption in HEK 293 cells. It was not always possible to track mitochondria for the entire duration of the acquired microscopy images (600 frames or 3 min) so here we present the actual lengths of the acquired trajectories. (a) Control (unperturbed) cells; (b) Cells exposed to 5 µM nocodazole for 4 h; and (c) Cells exposed to 10 µM nocodazole for 4 h. The results are presented both in terms of frames (lower *x* axes) as well as time (upper *x* axes). The number of trajectories is also specified for each condition.

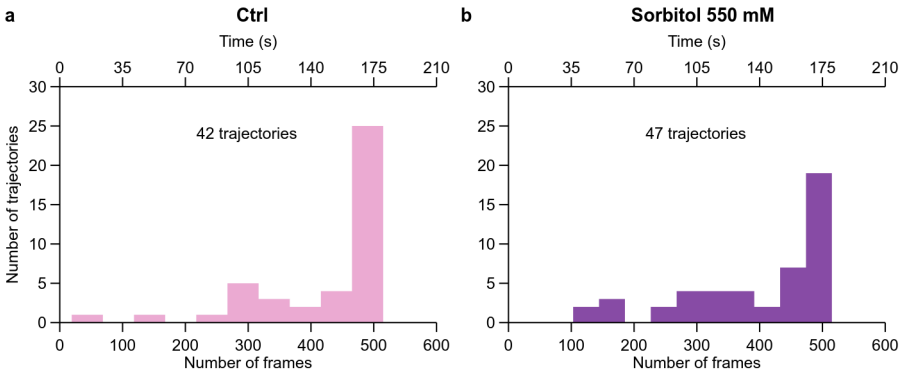

Figure S3. Trajectory length distributions of tracked mitochondria after crowding in HEK 293 cells. It was not always possible to track mitochondria for the entire duration of the acquired microscopy images (515 frames or 3 min) so here we present the actual lengths of the acquired trajectories. (a) Control (unperturbed) cells; and (b) Cells exposed to 550 mM sorbitol. The results are presented both in terms of frames (lower *x* axes) as well as time (upper *x* axes). The number of trajectories is also specified for each condition.

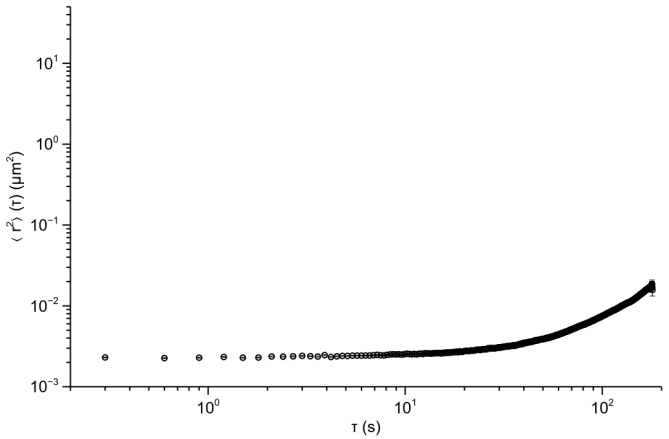

Figure S4. Mean square displacement of mitochondria in fixed HEK 293 cells. As a control for mitochondrion localisation precision, thermal diffusion, and drift of the microscope stage, the cells were fixed, the mitochondria tracked, and the ensemble- and time-averaged mean square displacement evaluated.

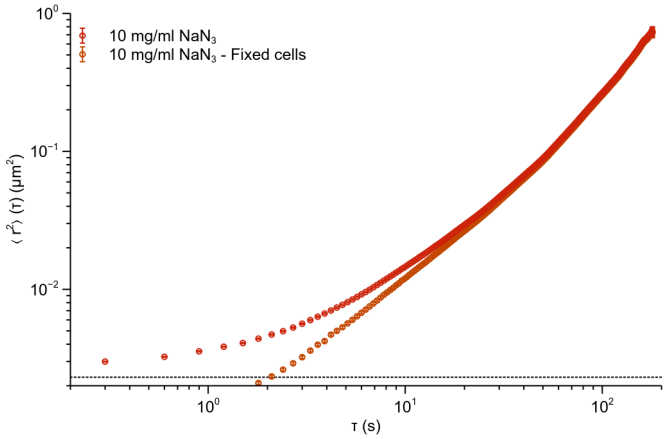

Figure S5. Effect of background movement on the ensemble- and time-averaged mean square displacement of mitochondria in HEK 293 cells. As a control for mitochondrial localisation precision, thermal diffusion, and drift of the microscope stage, we used mitochondria in fixed cells (Supplementary Fig. S4). To demonstrate that this background movement is negligible for the movement in living cells, we used the mean square displacement of mitochondria which moved the least (cells exposed to 10 mg/ml NaN_3, reproduced from Fig. 3c). When subtracting the background movement from these results, there is essentially no difference for timescales larger than 1–2 s. Conversely, at shorter timescales we reach the limit corresponding to localisation precision (the dotted grey line corresponds to the lowest value for the background movement; Supplementary Fig. S4).

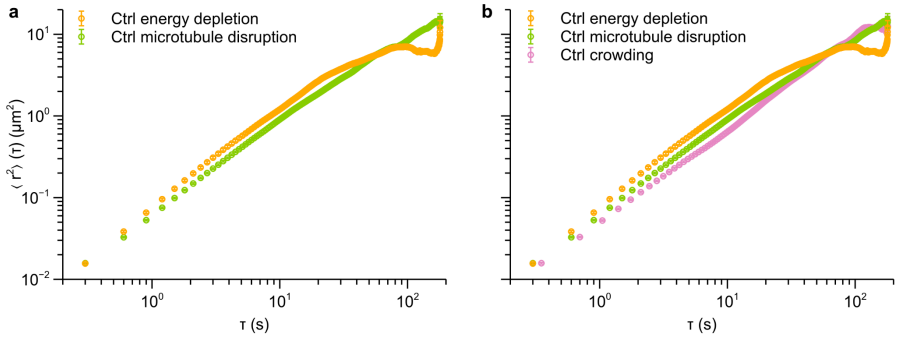

Figure S6. Comparison of mean square displacement of mitochondria from different experiments. We acquired three datasets of mitochondria in unperturbed HEK293 cells: one for the experiments on cell energy depletion; one for the experiments on microtubule disruption; and one for the experiment on crowding. In the case of the crowding experiments, we used stably transfected Flp-in T-Rex293 cells conditionally expressing the green fluorescent protein AcGFP1, which are strictly speaking not HEK 293 cells but are derived from them. (a) Comparison of the ensemble- and time-averaged mean square displacement of the two datasets from HEK 293 cells proper. There is excellent overlap between the two experiments at the shortest timescale and an overall reasonable agreement. The curves mainly differ at longer time scales, where the statistics get poorer. Some variability might be due to the different number of trajectories used for the analysis (Supplementary Fig. S1a and Supplementary Fig. S2a). (b) Comparison of all datasets, including the AcGFP1-expressing HEK 293 cells. There is still good agreement, though not as good as between the two HEK 293 cells proper (panel a).

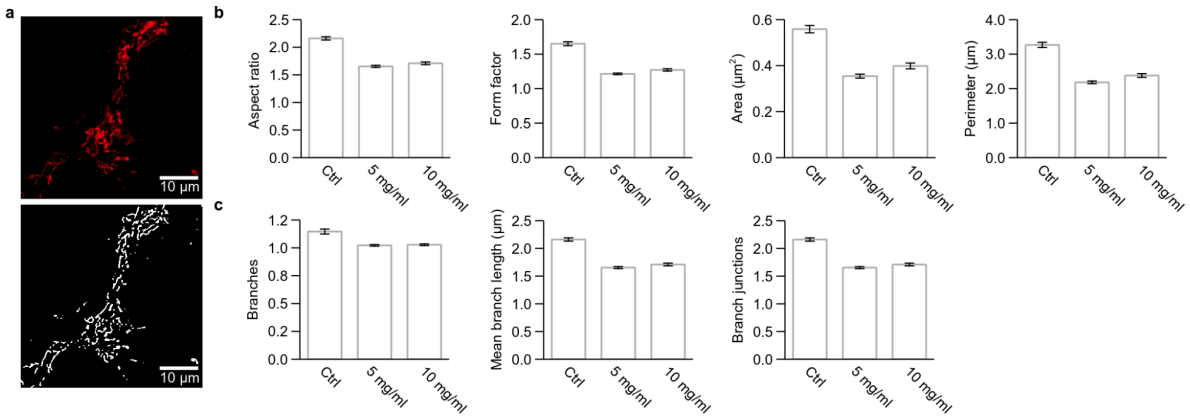

Figure S7. Mitochondrial network analysis of cell energy-depleted HEK 293 cells. (a) Before analysing the network (using the ImageJ Mitochondria Analyzer plugin[1] as described in the Supplementary Methods section), the (Top) original image of MitoTracker-stained mitochondria was thresholded into a (Bottom) binary image. (b) Morphological descriptors; and (c) network descriptors, depicting changes to the mitochondrial network before (Ctrl) and after exposure to sodium azide (5 and 10 mg/ml). 6 images per condition, amounting to approximately 1 000 mitochondria in total, were analysed. The bar graphs represent the mean ± standard error of the mean over mitochondria.

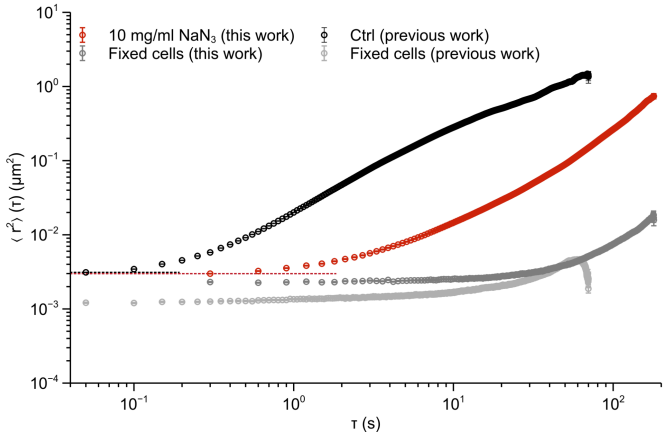

Figure S8. Potential plateau at short timescales for the mean square displacement of mitochondria in HEK 293 cells. Under energy-depleted conditions (NaN_3 10 mg/ml; results reproduced from Fig. 3c) there is the introduction of what appears to be a plateau at subsecond timescales (dotted line shows the mean square displacement at the shortest evaluated time as a guide to the eye). These results are close to the mean square displacement in fixed cells (reproduced from Fig. 3c or Supplementary Fig. S4), making it difficult to draw firm conclusions. However, in a previous work,[3] we have studied the motion of mitochondria, using a different experimental set-up (including a different microscope and faster acquisition) leading to a substantially lower mean square displacement in fixed cells. Despite the implied better localisation precision, the apparent plateau remains. It should be noted, though, that these results are for unperturbed cells.

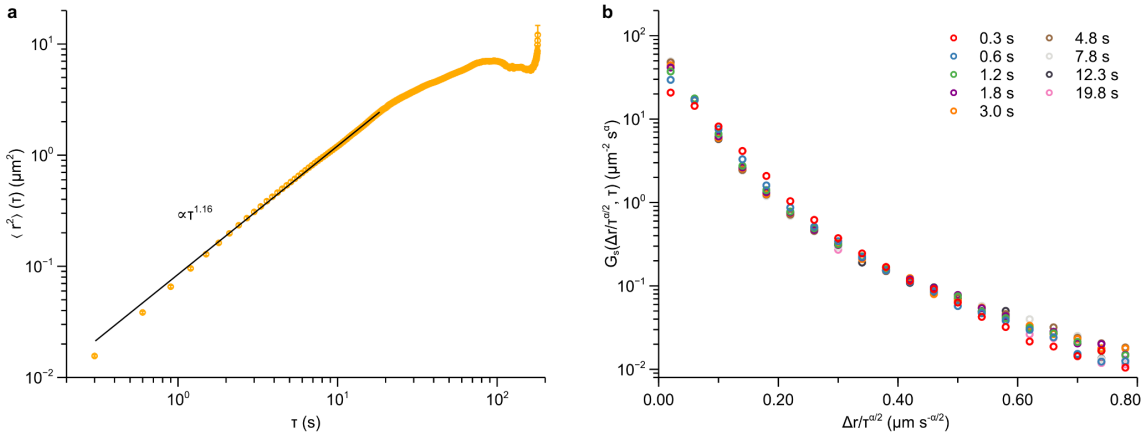

Figure S9. Collapse of the displacement distribution of mitochondria in (unperturbed) HEK 293 cells. a, The mean square displacement is roughly linear up to 20 s with an exponent α~1.16 (solid line shows a fit). Same data as shown in Fig. 3c; Ctrl. **b,** Using the exponent, α, evaluated from the mean square displacement to rescale the displacements by $\tau^{\alpha/2}$ shows that the displacement distributions roughly collapses to a universal function throughout the same time interval. The units of s^{α} for the displacement distribution (as opposed to the units of $s^{\alpha/2}$ on the *x* axis) arise from that we have excluded the factor $2\pi(r/\tau^{\alpha/2})$ that stems from the two-dimensional geometry throughout this work (*cf.* Fig. 4 and Supplementary Fig. S11 and S13). Same (underlying) data as Fig. 4.

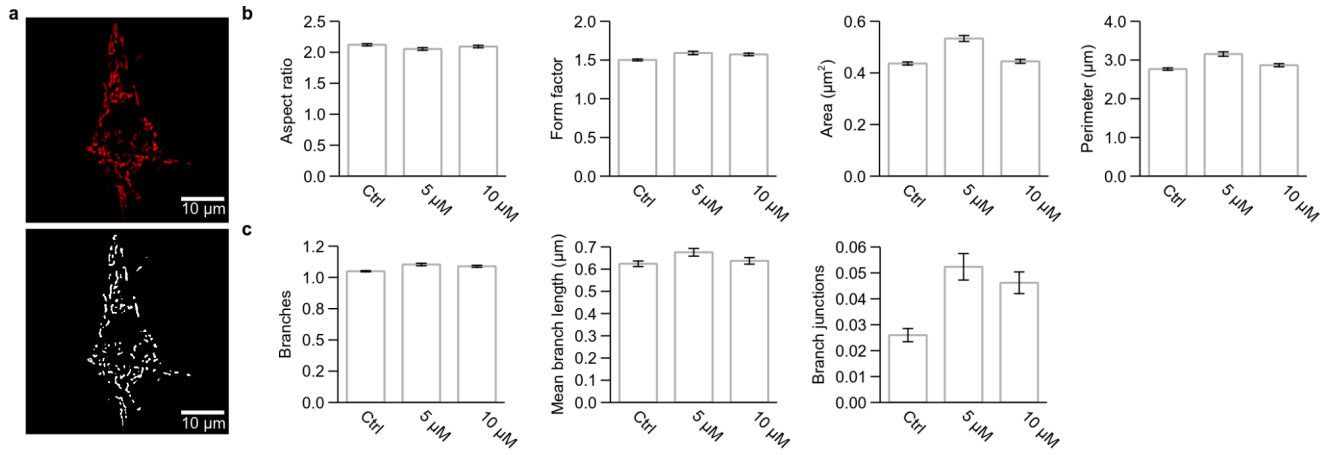

Figure S10. Mitochondrial network analysis after microtubule disruption in HEK 293 cells. (a) Before analysing the network (using the ImageJ Mitochondria Analyzer plugin[1] as described in the Supplementary Methods section), the (Top) original image of MitoTracker-stained mitochondria was thresholded into a (Bottom) binary image. (b) Morphological descriptors; and (c) network descriptors, depicting changes to the mitochondrial network before (Ctrl) and after exposure to nocodazole (5 and 10 µM). 6 images per condition, amounting to approximately 1 000 mitochondria in total, were analysed. The bar graphs represent the mean ± standard error of the mean over mitochondria.

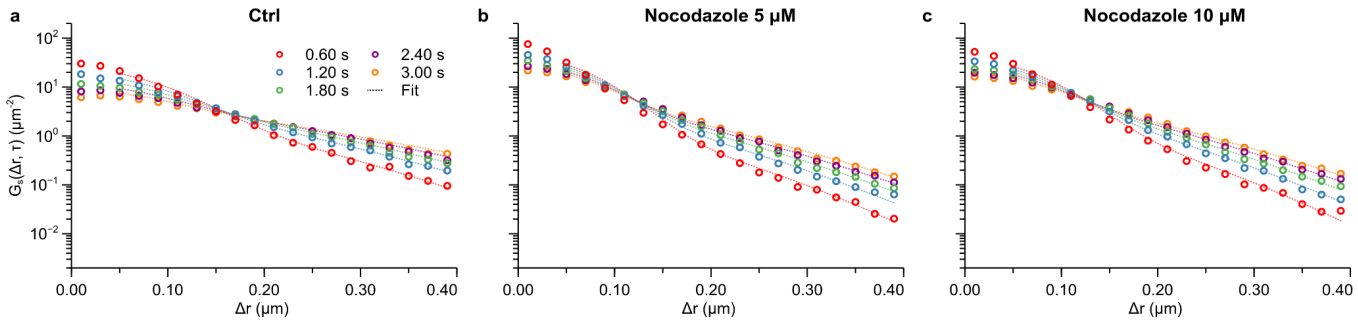

Figure S11. Displacement distribution of mitochondria after microtubule disruption in HEK 293 cells. Displacement distribution in (a) control cells (no microtubule disruption), together with cells where the microtubules have been disrupted by exposure to (b) 5 µM, and (c) 10 µM nocodazole for 4 h. In unperturbed cells, mitochondria show a high probability to move shorter distances around 0.05–0.10 µm, while the probability decreases for longer distances (Ctrl). After microtubule disruption, the probability that a mitochondrion will move longer distances becomes even smaller, meaning that fewer mitochondria move that far (Nocodazole 5 and 10 µM). A previously presented model describing the motion in several glassy systems[4,5] was globally fitted to the data for displacements larger than 0.05 µm (dashed lines) with the resulting fitting parameters reported in Table 2.

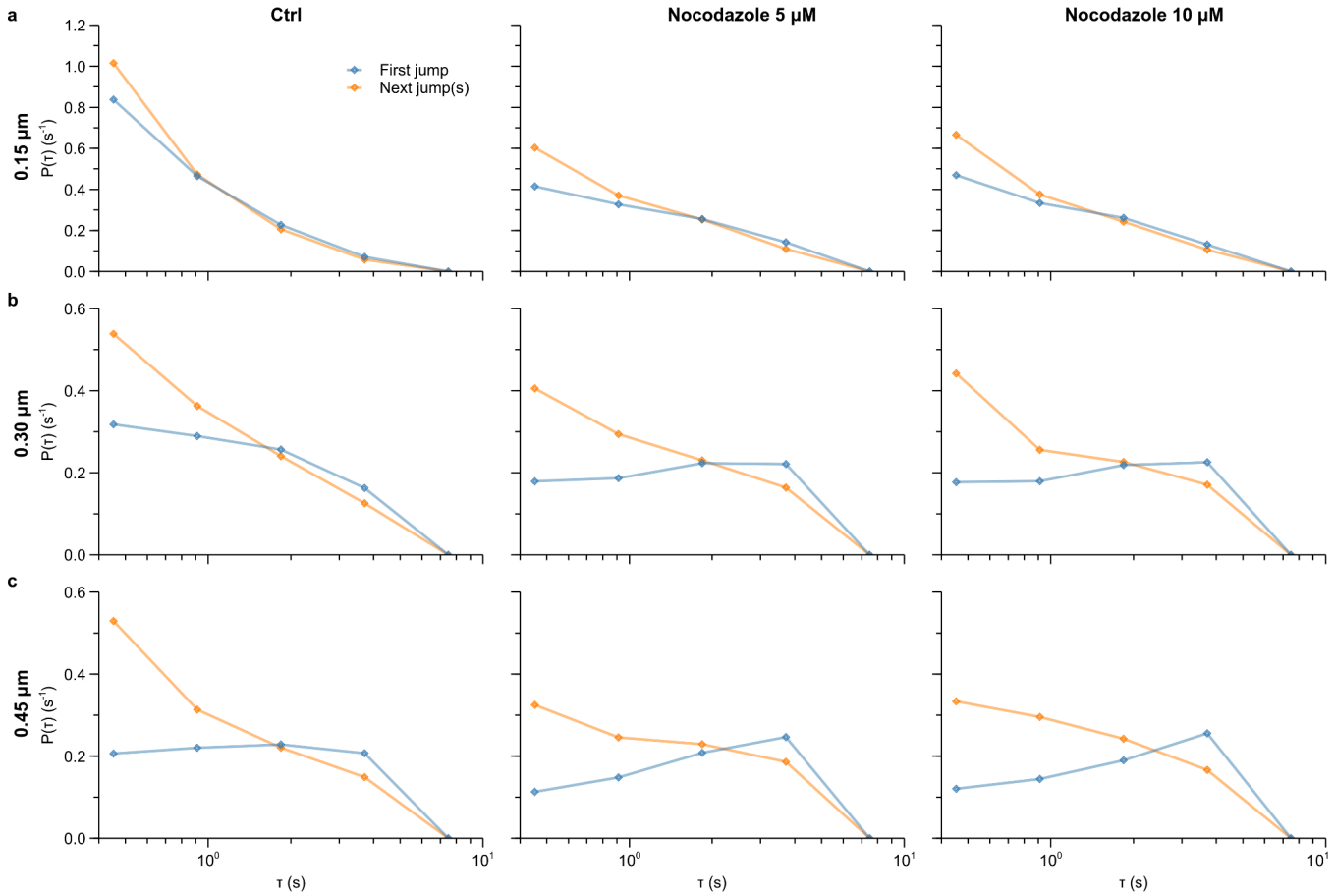

Figure S12. Waiting time distributions of mitochondria to move a given distance in microtubule-disrupted HEK 293 cells. The time before moving a certain distance the first time (blue) and any subsequent time (orange) was evaluated for distances of (a) 0.15 µm; (b) 0.30 µm; and (c) 0.45 µm. The results are presented in terms of the normalised probability density function of the two times. Note the log scale. The calculations were limited to the first 10 s only (see Experimental section in the main text for details). The data for unperturbed cells from this experiment (Ctrl) show a good agreement with the data from unperturbed cells in the cell energy-depletion experiment (Fig. 5; Ctrl) for all the three selected distances. Comparing unperturbed cells (Ctrl) with cells where the microtubules have been disrupted (Nocodazole 5 and 10 µM), shows a substantial increase both in the waiting time before a mitochondrion moves the distance the first time (blue data points) and a subsequent time (orange data points). Naturally, this is particularly so for longer distances (comparing 0.15 to 0.30 or 0.45 µm).

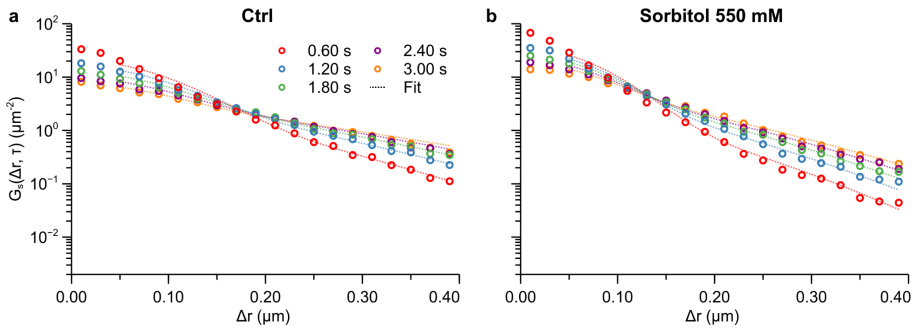

Figure S13. Displacement distribution of mitochondria in crowded HEK 293 cells. Displacement distribution in (a) control cells (not subjected to any perturbation), together with (b) cells crowded from exposure to 550 mM sorbitol. The results show that the probability that mitochondria move longer distances decreases upon crowding, as may be observed from the lower values of the distributions at short distances and higher values at the tails for unperturbed cells (Ctrl; data points) compared to the higher values of the distributions at short distances and lower values at the tails for crowded cells (Sorbitol 550 mM; data points). A previously presented model describing the motion in several glassy systems[4,5] was globally fitted to the data for displacements larger than 0.05 μm (dashed lines) with the resulting fitting parameters reported in Table 3.

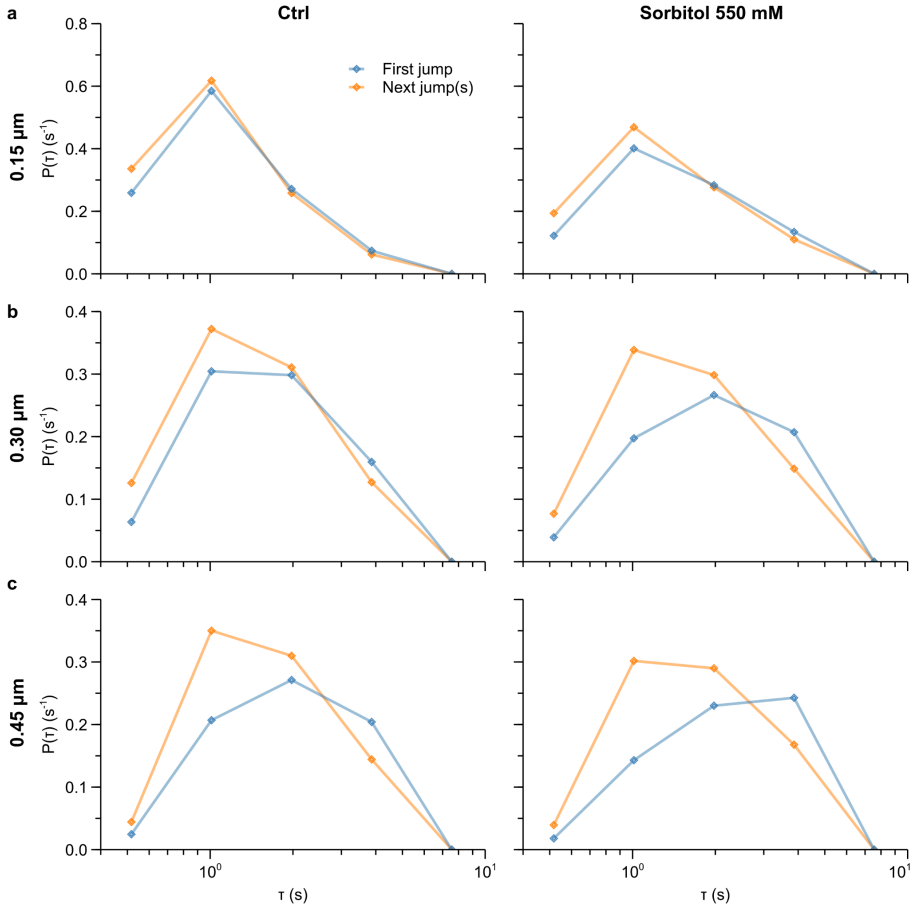

Figure S14. Waiting time distributions of mitochondria to move a given distance in crowded HEK 293 cells. The time before moving a certain distance the first time (blue) and any subsequent time (orange) was evaluated for distances of (a) 0.15 µm; (b) 0.30 µm; and (c) 0.45 µm. The results are presented in terms of the normalised probability density function of the two times. Note the log scale. The calculations were limited to the first 10 s only (see the Experimental section in the main text for details). The distributions for unperturbed cells (Ctrl) are not entirely consistent with those observed previously (Fig. 5 and Fig. S12; Ctrl), highlighting that these cells are slightly different compared to those used for the cell depletion and microtubule disruption experiments. In terms of the effect of crowding, the mitochondria take longer before performing the distance (Sorbitol 550 mM) regardless of the distance considered.

Supplementary table

Table S1. Parameter describing mitochondrial motion in cell energy-depleted HEK 293 cells (supplementing Table 1). The fits described in Fig. 4 and Table 1 did not result in a well-determined τ_2 parameter. To avoid confusion it is consequently not shown in Table 1, but is included here for completeness.

Condition	τ_2 **(s)**
Control	3.53 ± 2.70
5 mg/ml NaN_3	24.51 ± 34.42
10 mg/ml NaN_3	5.09 ± 1.19

Supplementary movie

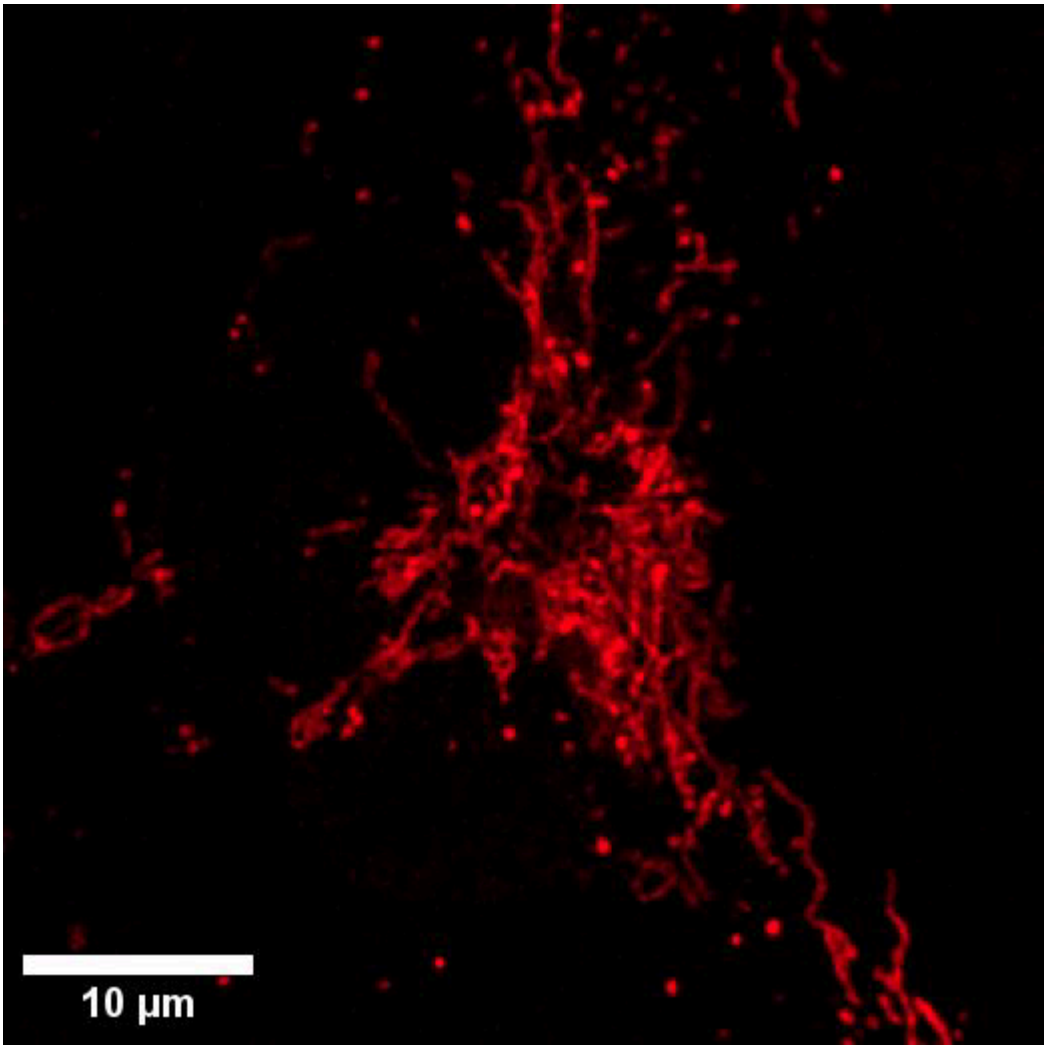

Movie S1. Mitochondria in HEK 293 cells. Mitochondria in HEK 293 cells were fluorescently labelled with MitoTracker Deep Red and observed live using confocal microscopy. One (two-dimensional) image was acquired every 300 ms for a total of 3 min. Note that the movie is subsequently sped up compared to real time. The punctuate (or spot-like) detached mitochondria were subsequently tracked as described in the Experimental section of the main text.

Supplementary references

1 A. Chaudhry, R. Shi and D. S. Luciani, *Am. J. Physiol.-Endocrinol. Metab.*, 2020, **318**, E87–E101.
2 I. M. G. M. Hemel, B. P. H. Engelen, N. Luber and M. Gerards, *Mitochondrion*, 2021, **59**, 216–224.
3 B. Corci, O. Hooiveld, A. M. Dolga and C. Åberg, *Soft Matter*, 2023, **19**, 2529–2538.
4 P. Chaudhuri, L. Berthier and W. Kob, *Phys. Rev. Lett.*, 2007, **99**, 060604.
5 P. Chaudhuri, Y. Gao, L. Berthier, M. Kilfoil and W. Kob, *J. Phys. Condens. Matter*, 2008, **20**, 244126.